Biomed Tech 2008; 53:52–58 © 2008 by Walter de Gruyter • Berlin • New York. DOI 10.1515/BMT.2008.006

Inverse finite element characterization of the human myometrium derived from uniaxial compression experiments

Von einaxialen Druckversuchen hergeleitete inverse Finite-Elemente-Charakterisierung des menschlichen Myometriums

Stephan Weiss[1,*], Peter Niederer[1], Alessandro Nava[2], Rosmarie Caduff[3] and Michael Bajka[4]

[1] Institute for Biomedical Engineering, University and ETH Zurich, Zurich, Switzerland
[2] Centre of Mechanics, ETH Zurich, Zurich, Switzerland
[3] Institute of Surgical Pathology, University Hospital of Zurich, Zurich, Switzerland
[4] Clinic of Gynecology, Department OB/GYN, University Hospital of Zurich, Zurich, Switzerland

Abstract

The low strain-rate behavior of the human myometrium under compression was determined. To this end, uniaxial, unconstrained compression experiments were conducted on a total of 25 samples from three excised human uteri at strain rates between 0.001 s^{-1} and 0.008 s^{-1}. A three-dimensional finite element model of each sample was created and used together with an optimization algorithm to find material parameters in an inverse estimation process. Friction and shape irregularities of samples were incorporated in the models. The uterine specimens in compression were modeled as viscoelastic, non-linear, nearly incompressible and isotropic continua. Simulations of uniaxial, frictionless compressions of an idealized cuboid were used to compare the resulting material parameters among each other. The intra- and inter-subject variability in stiffness of specimens was found to be large and to cover such a wide range that the effect of anisotropy which is of minor influence under compressive deformations in the first place could be neglected. Material parameters for a viscoelastic model based on a decoupled, reduced quadratic strain-energy function were presented for the uterine samples representing a median stiffness.

Keywords: compression experiment; compressive behavior; inverse finite element; myometrium; uterus.

Zusammenfassung

Diese Studie hatte zum Ziel, das Verhalten von menschlichem Myometrium bei geringen Dehnungsgeschwindigkeiten unter Kompression zu bestimmen. Dazu führten wir einaxiale Druckversuche an 25 Proben von 3 exzidierten Uteri mit niedrigen Dehngeschwindigkeiten zwischen 0,001 s^{-1} und 0,008 s^{-1} durch. Von jeder Probe wurde ein dreidimensionales Finite-Elemente-Modell erstellt, und mit einem inversen Optimierungsalgorithmus konnten daraus Materialparameter bestimmt werden. Unregelmäßigkeiten der Probengeometrie und die Reibung zwischen Probe und Platten fanden im Modell Berücksichtigung. Die Uterusproben wurden als viskoelastische, nicht-lineare, fast inkompressible und isotrope Kontinua modelliert. Die resultierenden Materialparameter wurden anhand von Simulationen einaxialer, reibungsfreier Druckversuche an einer idealisierten rechteckigen Probe untereinander verglichen. Die Resultate zeigten eine enorme Variabilität bezüglich der Steifigkeit sowohl innerhalb eines Organs als auch zwischen verschiedenen Uteri. Das Ausmass der Variabilität der Parameterwerte war so groß, dass der Einfluss der Anisotropie, welcher unter kompressiver Belastung ohnehin gering ist, vernachlässigt werden konnte. Schliesslich wurden Materialparameter von Samples mit einer medianen Steifigkeit präsentiert. Diese Parameter beschrieben ein viskoelastisches Modell, das auf einer entkoppelten, reduzierten, quadratischen Verzerrungsenergie-Funktion basiert.

Schlüsselwörter: Druckversuch; inverse finite Elemente; Myometrium; Uterus; Verhalten unter Kompression.

Introduction

The human uterus is a fibro-muscular organ divided into an upper part (uterine body, corpus) and a lower constricted segment (cervix). The arched part of the uterine body that covers the entry of the fallopian tubes into the uterus is referred to as the fundus of the uterus. The uterine wall, which is approximately 1–2 cm thick, is composed of three layers: the endometrium (mucosal layer, tapering the uterine cavity), the perimetrium (covering layer of the intra-abdominally part of the uterus, corresponding to the peritoneum), and between these two layers, the myometrium. The myometrium is by far the thickest layer, consisting of smooth muscle bundles and connective tissue, particularly containing collagen fibers.

In gynecology, a number of minimally invasive procedures are performed on the uterus, which requires training and experience. Attempts are therefore made to develop computer-controlled simulators for training purposes [20]. To convey a realistic impression to the user,

*Corresponding author: Stephan Weiss, Institute for Biomedical Engineering, University and ETH Zurich, Gloriastrasse 35, CH-8092 Zurich, Switzerland
Phone: +41-1-632-27-94
Fax: +41-1-632-11-93
E-mail: weiss@biomed.ee.ethz.ch

not only the anatomical details but also the mechanical behavior of the uterine tissue has to be known and implemented in the simulation.

Several types of mechanical experiments on the uterine organ have been performed *in vivo* [10–13] and *in vitro* [3–5, 17, 18, 25] over the last decades. Recently, Kauer et al. [12] determined parameters for a viscoelastic material model based on continuum mechanics from aspiration experiments on the combined myometrium and perimetrium, where the uterine tissue under examination was mostly in tension.

Uniaxial, unconstrained compression experiments are common and widely used to test and characterize soft tissue [2, 14, 17, 22], although they are associated with a number of drawbacks. First, boundary conditions are not well defined because of the friction between the platens used for compression; second, a non-uniform deformation pattern is observed, in particular when large deformations are attempted. On the one hand, the assumption of a frictionless interaction between the platens and an idealized cylinder or cuboid in compression may lead to an analytical solution of the stress-strain relation (assuming incompressibility and isotropy). On the other hand, the friction phenomenon in unconfined compression on soft tissues can considerably influence the resulting stress-strain relation and has to be taken into account [14, 26, 27]. To avoid this problem, the bottom and top surfaces of the test cylinder can be glued to the platens which simplifies the analysis of the stress-strain relation for nominal strains up to 30% [14] (assuming idealized geometries). Furthermore, due to shape irregularities, an analytical solution of the stress-strain relation for a given hyperelastic problem is not possible. Instead, an inverse finite element (FE) method can be used to approximate the exact solution [12, 15].

Biological soft tissue exhibits time-dependent effects (e.g., stress relaxation and creep), with behavior that depends on the stress history [6]. In the past, the relaxation phenomenon of the human myometrium has been described by means of uniaxial elongation experiments [4], but no material parameters for a continuum mechanics approach were presented.

Therefore, the aim of this project was to determine material parameters for the human myometrium at low compressive strain rates and during relaxation, thereby taking into account both friction between the sample and the platens, as well as shape irregularities of cylindrical samples.

Our results yielded information about the quasi-static and low strain-rate behavior of the human myometrium in compression. Isotropic material properties were thereby assumed, although the fibrous nature of the uterine material suggests some anisotropic behavior. Anisotropy was, however, neglected mainly for two reasons. First, under compressive strain, the isotropic quasi-incompressible matrix represents the main load-bearing structure, while the fibers exhibit a rather tortuous shape and can be expected to contribute only marginally to the mechanical properties under these conditions. At equivalent strains, the stiffness of the myometrium in compression is in fact considerably lower than in tension [17], a finding which we attribute to the deformation and loading characteristics of the collagen and muscle fibers. Accordingly, under the assumption of a minimal contribution of these fibers to the stiffness of the myometrium in compression, the results are of use to characterize a transversely isotropic hyperelastic material model [19] for the myometrium, consisting of an isotropic matrix where the fiber structure exerts its influence mainly under tension. Second, the results show an enormous spread of the constitutive parameters. This spread considerably exceeds the variability of mechanical properties which is often encountered in biological materials. This can be explained from the fact that the uterus undergoes significant changes during the menstrual cycle, after the menopause and in particular during pregnancy. Furthermore, the uterus lacks its major purpose during non-pregnancy. Accordingly, the muscle fibers show minimal activity and their architecture may exhibit a large variability. Taking into account anisotropy would on the one hand increase the number of parameters to be determined and thereby increase the critically conditioned nature of the problem. On the other hand, the (small) influence of anisotropy (under compression) would largely be blurred and not become evident within the general wide range of the parameter values.

Materials and methods

Samples

With clinical biopsy punches (8.0 mm ∅), a total of 25 samples were taken from three *ex vivo* organs of Caucasian patients (Table 1, uteri 1–3) subjected to hysterectomy for non-tumorous indications. Experiments were approved by the Swiss Ethics Review Board (KEK SPUK GGU), and informed written consent was obtained from the patients. The samples were cut out of healthy parts of the corpus, fundus and cervix of the uteri. Additionally, one specimen was cut out of a myoma of uterus 2 (Table 1). The bottom and top surfaces of the samples were prepared with a scalpel, removing the perimetrium and endometrium completely, resulting in sample heights

Table 1 Clinical data.

Uterus number	Age	Given births	Lost pregnancies	Indication for surgery	Hormonal replacement therapy	Samples (n)
1	43	1	1	Myomas with dysmenorrhea	No	8
2	50	0	0	Myomas with bleeding disorders	No	10
3	38	3	0	Myomas with dysmenorrhea and bleeding disorders	No	7

between 3.4 and 6.5 mm. The specimens were wrapped in cloth soaked with isotonic sodium chloride and stored in a refrigerator for a maximum of 5 h.

Experimental setup

Samples were mounted for testing in a universal uniaxial test machine (Zwick Z2.5, Zwick 1456, Zwick Inc., Ulm, Germany) between two polyvinyl chloride (PVC) platens (20 mm ∅). The deformation process was recorded by a digital camera mounted perpendicularly to the loading axis. Image sequences were recorded at frame rates of 5 fps and 10 fps for low (0.5 mm/min) and higher (1 mm/min) speeds of the upper platen, respectively. Samples were not preconditioned and were compressed to approximately half of their initial length at nominal strain rates between $\dot{\varepsilon}=0.001$ s^{-1} and $\dot{\varepsilon}=0.008$ s^{-1}. Afterwards, the position of the upper platen was kept constant for approximately 600 s (relaxation). All compression experiments were performed at room temperature (25°C).

Sliding between the platens during compression was observed for all samples. The coefficient of friction between the myometrium and the platens was estimated by sliding experiments. For these tests, 46 cubic strips were cut out of another three uteri (uteri 4–6) and stored the same way as described above. The samples were then pressed against a dry PVC plate by weights resulting in a pressure of approximately 5 kPa and dragged over a distance of 5 cm. The maximal friction force was thereby measured with a spring scale (resolution 2.5×10^{-3} N) from which the maximal friction coefficient of sliding μ could be determined.

Soft tissue model

To account for the large strains that occurred under compression, a non-linear hyperelastic material law was chosen [9, 16]. The uterine tissue model was assumed to be homogeneous, isotropic and nearly incompressible. The following decoupled, reduced quadratic form of the strain-energy function depending on the reduced invariants $\bar{I}_1=I_1(\bar{\mathbf{C}})$, $\bar{I}_2=I_2(\bar{\mathbf{C}})$ and $J=\sqrt{(I_3(\mathbf{C}))}$ of the right Cauchy-Green tensor $\mathbf{C}$ with the material parameters c_1, c_2 and $\kappa=10^7$ MPa (nearly incompressible material) was used:

$$\Psi=\Psi_{iso}(\bar{I}_1)+\Psi_{vol}(J)=c_1(\bar{I}_1\text{-}3)+c_2(\bar{I}_1\text{-}3)^2+\frac{9}{2}\kappa(J\text{-}1)^2. \quad (1)$$

For $c_1\geq0$ and $c_2\geq0$, the proposed strain-energy function is proven to be polyconvex and coercive, which is sufficient to guarantee a solution for all boundary conditions and body forces [8].

The time-dependent (viscoelastic) effects of the uterine tissue were modeled with a quasi-linear approach [21]. The second Piola-Kirchoff stresses $\mathbf{S}(t)$ at time t were additively composed of a quasi-static part $\mathbf{S}^\infty$ and a part incorporating the history dependence of the stresses,

$$S(t)=S^\infty(C(t))+\sum_{i=1}^{3}\delta_i\int_0^t\frac{\partial}{\partial s}S^e(C(t))\exp\left(\frac{-(t\text{-}s)}{\tau_i}\right)ds \quad (2)$$

where $S^e=2\dfrac{\partial\Psi(C)}{C}$ is the instantaneous and $S^\infty=\left(1\text{-}\sum_{i=1}^{3}\delta_i\right)S^e$ the quasi-static response to a given deformation. Therefore, the weighting factors δ_i are constraint to

$$\delta_i\geq0 \quad (3)$$

and

$$\sum_{i=1}^{3}\delta_i\leq1. \quad (4)$$

Furthermore, the relaxation times are required to be positive:

$$\tau_i\geq0 \quad (5)$$

The relaxation times τ_i characterize the decay time and the corresponding weighting factors δ_i the amount of decay of the stress response. Therefore, for every compression experiment, the eight parameters $\mathbf{p}=\{c_1, c_2, \delta_1, \delta_2, \delta_3, \tau_1, \tau_2, \tau_3\}$ had to be determined. The Cauchy stresses $\boldsymbol{\sigma}(t)$ can be calculated according to $\boldsymbol{\sigma}=J^{-1}\mathbf{FSF}^T$, where $\mathbf{F}$ is the deformation gradient and $\mathbf{F}^T$ the transposed deformation gradient.

Finite element model

The camera data were synchronized with the time-displacement-force data of the uniaxial test machine according to the movement of the upper platen. The stress- and strain-free configuration of the samples was defined as the first incident where the recorded force increased above the medium noise level of the force sensor ($\sim10^{-3}$ N). On the recorded picture, the upper platen normally touched the samples on a small area (Figure 1A). A two-dimensional contour formed by the projection of the sample in the image plane was extracted semi-automatically. Using a custom algorithm, two points p_n and p_{n+1} on the same z height were then rotated around their common center m (Figure 1B), which resulted in a point cloud (approximately 120,000 points) that was not axially symmetric, but whose projection onto the y-z plane corresponded to the two-dimensional picture of the sample in the stress-free configuration (Figure 1C). A commercially available software package (Raindrop® Geomagic® 7.0, Research Triangle Park, NC, USA) was used to wrap the points into a triangular surface mesh consisting of an arbitrary number of triangles. A three-dimensional tetrahedral FE mesh was created thereafter with the automatic mesh generator of the software package MSC.Marc® Mentat® 2005 R2 (Santa Ana, CA, USA) (Figure 1D). The resulting mesh was then scaled according to the displacement data of the uniaxial compression test machine (from pixel to mm). For every sample, an FE mesh consisting of approximately 3000 low-order

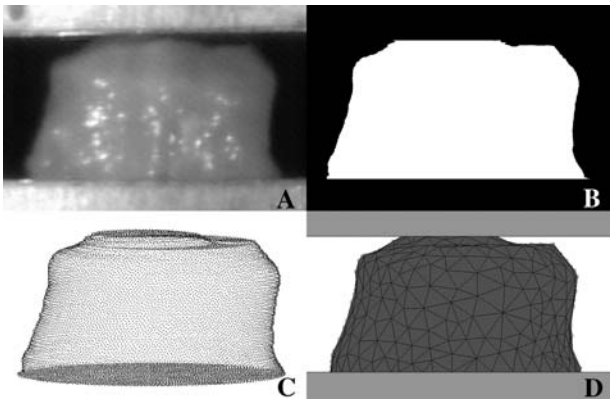

Figure 1 Finite element mesh creation.
(A) Digital image of a sample of the uterine myometrium in the assumed stress- and strain-free configuration. The distance between the compression platens is 5.02 mm. (B) Extracted contour of the sample in (A). Two points p_n and p_{n+1} at every z level are rotated around their common center m which results in a point cloud (C), which is wrapped in triangular surface and meshed into a three-dimensional tetrahedron mesh (D) of (A).

tetrahedrons was constructed in the manner described above. To examine the sensitivity of results to mesh discretization, three additional, finer meshes (12,000, 45,000 and 106,000 tetrahedrons) of one sample were created. Finally, the two platens were introduced into each FE model. The material behavior of the uterine samples was modeled according to the hyper- and viscoelastic strain-energy function described above. Sample/platens friction was assumed to be of coulomb type (arctan model in MSC.Marc® 2005 R2).

Using these non-linear FE models, the complete set of compression experiments were computed in 100 time steps (20 steps during compression and 80 steps during relaxation) by the software package MSC.Marc® 2005 R2.

Inverse finite element parameter estimation

An inverse FE estimation consists of the simulation of a real physical problem with the help of an FE model whose parameters are varied according to a systematic algorithm until the simulated and the experimental data are sufficiently well matched. Here, as error function to be minimized, the expression

$$error(\mathbf{p}) = \sum_{i=1}^{100} \left(force(i)_{\exp} - force_{sim}(i)\right)^2$$ with the parameter set

$$\mathbf{p} = \{c_1,\ c_2,\ \delta_1,\ \delta_2,\ \delta_3,\ \tau_1,\ \tau_2,\ \tau_3\}$$

was used whereby $force(i)_{sim}$ and $force(i)_{\exp}$ were the forces measured at the moving platen at time step i of the simulation and experiment, respectively. As optimization algorithm, the Matlab function lsqnonlin (Matlab® 7, R14 SP3, Natick, MA, USA) was applied. The set of parameters **p** that minimized the error function was assumed to characterize the observed behavior of the uterine tissue sample during the described experiment sufficiently well.

The reliability of the parameters $\mathbf{p} = \{c_1,\ c_2,\ \delta_1,\ \delta_2,\ \delta_3,\ \tau_1,\ \tau_2,\ \tau_3\}$ was determined according to a parameter sensitivity analysis, where a variation of a parameter (e.g., 11.35 kPa to 11.44 kPa for the final value 11.4 kPa) resulted in a change of the squared correlation (R^2) between the experiment and the simulation by less than 0.05% compared to that obtained using the resulting parameters from the inverse FE algorithm.

Comparison of parameters

As the samples used in the experiments had various shapes, the parameters obtained by the inverse FE method were compared on the basis of simulated uniaxial compression "tests". All of the samples were thereby assumed to exhibit the same cylindrical shape and the friction between "platens" and sample was set to zero. The following strain history was applied: 125 s compression with a strain rate $\dot{\varepsilon} = 0.004\ s^{-1}$ and subsequent constant nominal strain of 50% for 875 s.

Results

For most of the samples, the maximal friction coefficient was found to fall between 0.04 and 0.12 (Figure 2) and was set to 0.1 for all FE calculations. In general, the friction force increased over the 5-cm distance of sliding due to a rarefaction of the fluid film between sample and plate.

All inverse FE simulations converged and fitted the experimental data very well (mean $R^2 > 0.98$) such that the eight parameters $\mathbf{p} = \{c_1,\ c_2,\ \delta_1,\ \delta_2,\ \delta_3,\ \tau_1,\ \tau_2,\ \tau_3\}$ could be determined for all samples. Theoretical uniaxial compression curves according to the procedure outlined in the above section on "Comparison of parameters" were then calculated on the basis of these parameters; the respective curves for each uterus are shown in Figures 3–5. All the curves are of a non-linear type showing a distinctive relaxation phenomenon. For the specimens of uterus 1, the maximal compressive Cauchy stress ranged between 10 kPa and 122 kPa (Figure 3). For the cervix, stresses were between 26 kPa and 54 kPa, while for uterus 2, the maximal values reached 3 kPa to 123 kPa (Figure 4) (3.3 kPa for the myomatous specimen). For those of uterus 3, peak stresses were between 3 kPa and 14 kPa (Figure 5) and between 3.5 kPa and 6.7 kPa for the corpus alone.

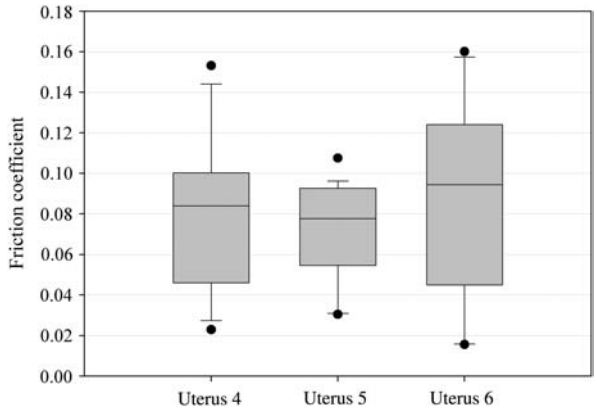

Figure 2 Maximal friction coefficients of uteri 4–6 (11, 17 and 18 samples) measured by sliding cubic stripes of myometrium on PVC over a distance of 5 cm.
Box plots show each outlier, 10, 25, 50, 75 and 90 percentiles.

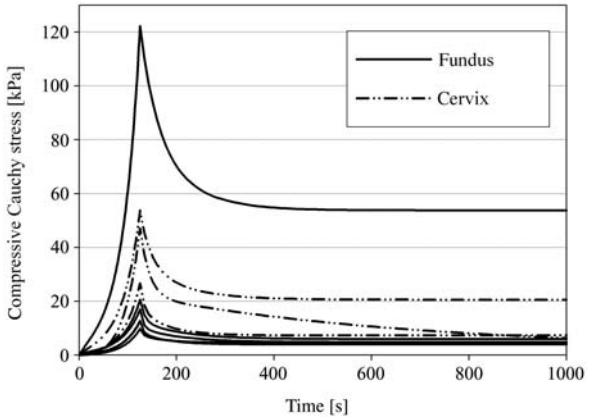

Figure 3 Compressive properties of eight samples from uterus 1 (Table 1).
The strain history is presented in the section on "Comparison of parameters" in the text.

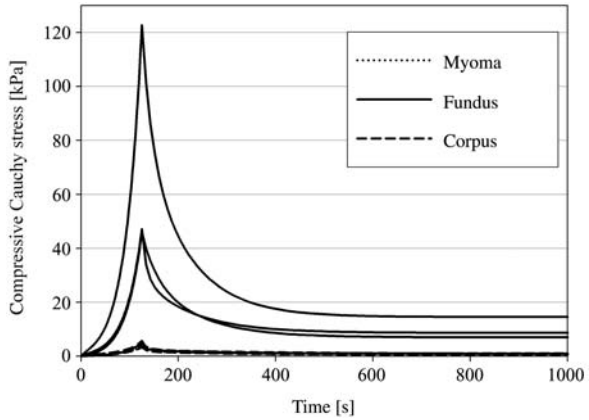

Figure 4 Compressive properties of ten samples from uterus 2 (Table 1).
The strain history is presented in the section on "Comparison of parameters" in the text. The three stiffest samples were taken from the fundus, whereas the curves from all other samples are not distinguishable on this scale.

For comparison purposes, for each uterus an exemplary curve was chosen. Thereby, $\mathbf{p}_1$ relates to the curve passing closest to the median of the calculated stress maxima of all the samples of uterus 1 (the 4th curve from above, Figure 3), $\mathbf{p}_2$ relates to the one of uterus 2 and $\mathbf{p}_3$ to the one of uterus 3 (Table 2). The large biological variability is clearly evident from these values. The strain rate dependency in compression of a material characterized by $\mathbf{p}_3$ (Table 2) is shown in Figure 6.

A FE calculation with three finer meshes (approximately 12,000, 45,000 and 105,000 tetrahedrons) of the particular sample characterized by $\mathbf{p}_3$ (Table 2) showed that the maximal force converged for each model did not change by more than 2.3%, indicating that the employed meshes were sufficiently adequate.

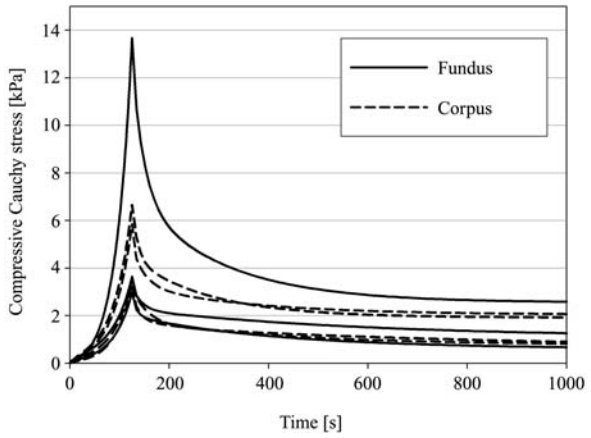

Figure 5 Compressive properties of seven samples of uterus 3 (Table 1).
The strain history is presented in the section on "Comparison of parameters" in the text.

Discussion

As can be observed in Figures 3–5, the intra- and inter-subject variability in stiffness of specimens was quite high, which was also indicated by the raw data of the uniaxial test machine. The peak compressive Cauchy stresses (strain history in the parameter comparison section) were found to fall between 3 kPa and 123 kPa. Kauer et al. [12] performed *in vivo* and *in vitro* aspiration experiments on the surface of uteri and presented material parameters for three *in vivo* and three *in vitro* measurements on a single uterus. Simulated compression (strain history in the parameter comparison section) based on these parameters lead to maximal Cauchy stresses between 23 kPa and 71 kPa. In this comparison, the aspiration technique employed by Kauer and the method presented here revealed results of the same order of magnitude, although the two methods are quite different. It should be noted, however, that non-linear curves are difficult to compare and a stress comparison at 50% nominal strain is somewhat arbitrary. Kauer et al. found a pronounced decrease in uterine stiffness between *in vivo* and *in vitro* measurements (performed approximately 30 min after excision), which could not be verified with the experiments presented here. In another set of experiments, Pearsall and Roberts [17] found in compression of the myometrium at strain rates between $\dot{\varepsilon}=0.008\ s^{-1}$ and $\dot{\varepsilon}=0.017\ s^{-1}$ Cauchy stresses between 7 kPa and 70 kPa at 50% nominal strain. They used specimens from the upper uterine wall and the fundus, whereas we tested samples from three substantially different parts of the organ.

In our experiments, samples excised from the fundus showed the most mechanical variability, exhibiting both the stiffest and softest behavior of all samples. Speci-

Table 2 Mechanical characterization of the human myometrium.

Uterus number	Parameter name	c_1 [kPa]	c_2 [kPa]	δ_1	δ_2	δ_3	τ_1 [s]	τ_2 [s]	τ_3 [s]
1	$\mathbf{p}_1$	8.2	10.0	0.578	0.291	0.080	0.01	9	83
2	$\mathbf{p}_2$	19	7.4	0.9005	0.0747	0.0165	0.05	10	134
3	$\mathbf{p}_3$	11.4	5.2	0.9409	0.0316	0.0149	0.2	19	470

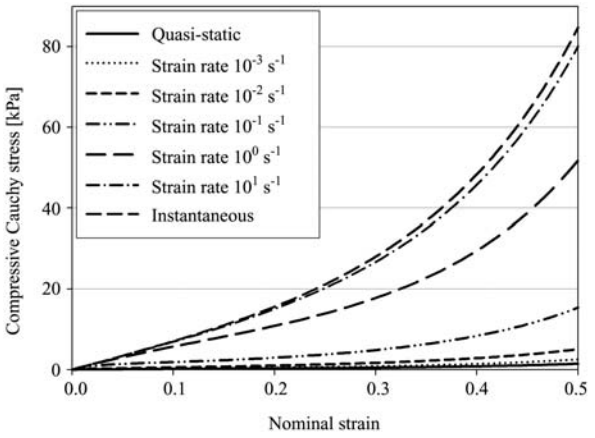

Figure 6 Strain rate dependence of a material under compression characterized by $\mathbf{p}_3$ (Table 2).
The faster this material is deformed, the more stiffly it behaves.

mens from the cervix and corpus showed somewhat less variability in stiffness. In the non-pregnant state, the uterus is devoid of its main function of fostering the fetus. Apart from spontaneous small uterine contractions, the uterus lacks major muscular activity for which there is no need. Some disorder in the uterine structure might therefore well be explicable. Water content is furthermore highly variable throughout the menstrual cycle. After the menopause, a gradual regressive development sets in, which is associated with further changes in the mechanical properties. For all of these reasons, a large variability of the mechanical behavior of uterine tissue which exceeds the typical variability found in other soft biological tissues by far is to be expected. A particular aspect is finally related to pathological processes, which are of importance from a clinical perspective. So far, only healthy samples were tested. Pathological structures will, however, introduce a further range of mechanical characteristics. Aiming at an FE simulation of hysteroscopy, which is of use for realistic training purposes, pathological changes have to be integrated locally into a model consisting of healthy tissue.

Using the inverse FE algorithm, we could not fit a neo-Hookean model ($c_2 = 0$ kPa) with six relaxation terms to the experimental data and therefore a second-order strain-energy function (Equation 1) was chosen. All the parameters affected both compression and relaxation phase of the simulation according to Equations 1 and 2. Furthermore, the relaxation terms were constraint to Equations 3, 4 and 5. Probably, these were the reasons that a minimum of six relaxation terms were needed for the inverse FE fits.

Because the samples were obtained with the aid of a biopsy punch in an essentially transmural direction, the loading axis of the uniaxial testing procedure was not aligned with a specific muscle fiber direction. Besides, the variability of the fiber direction field [7, 23, 24] within the volume of the samples would render such an alignment hardly possible. In principle, the fibrous nature of the material could be taken into account in the form of anisotropy of the model characteristics provided that the fiber architecture within the sample was known. In compression, however, the anisotropy due to the collagen and muscle fibers can be expected to be of minor importance, as the quasi-incompressible isotropic matrix represents the main structural element. In fact, the stiffness of the myometrium in compression is significantly lower than in tension at equivalent strains [17], which can be attributed, as outlined in the "Introduction" section, to the tendency of muscle and collagen fibers to buckle in compression. Therefore, the fiber architecture of the uterus is supposed to affect its mechanical behavior significantly in tension, but only marginally in compression. The presented material parameters can therefore be used for the characterization of an isotropic matrix of a transversely isotropic hyperelastic material model [19] for myometrium. To fully characterize the mechanical properties of the uterine tissue, contributions reflecting the fibers and the interaction between the fibers and the matrix have to be added which manifest themselves under tension.

The material parameters $\mathbf{p} = \{c_1, c_2, \delta_1, \delta_2, \delta_3, \tau_1, \tau_2, \tau_3\}$ of the model given above were determined with the help of low strain rate compression/relaxation experiments during approximately 600 s. For the purpose of surgery simulation, this limitation can be justified by the fact that rapid deformations are usually avoided, at best possible, in invasive procedures. An extrapolation to other loading situations, such as creep, high strain rate, torsion, long time ($\gg 600$ s), shear is possible but has to be treated with care. Furthermore, the parameters $\mathbf{p}$ were obtained by a minimization algorithm with which only local minima of the error function *error*($\mathbf{p}$) were found. Thus, the resulting parameters $\mathbf{p}$ may not be unique and other sets may lead to comparable accuracy in the low strain rate range.

Friction in general is a complex phenomenon and should not be neglected when testing soft tissue under uniaxial compression [14, 26, 27]. Gluing the samples to the platens would remove the issue of friction. Nevertheless, high shear stresses at the platen-sample contact may complicate the determination of material properties for nominal strains higher than 30% [14]. However, in the presented experiments, the nominal strains were as high as 50% and therefore the samples were not glued to the platens. The sample width at the lower platen was extracted from every picture as a measure of friction. But this method proved to be too sensitive and prone to errors. Therefore, the maximal friction coefficient was estimated from sliding experiments on a PVC plate over a length of 5 cm, where the samples were under a compressive pressure of approximately 5 kPa, which was comparable to the mean pressures of the compression experiments. The friction forces increased over distance probably due to dehydration at the contact surface of the samples. During the compression experiments, the samples slid only a few millimeters and therefore the friction coefficient of 0.1 represented an upper bound. The influence of the friction parameter μ on the simulated force-time curve of the sample characterized by $\mathbf{p}_3$ can be seen in Figure 7.

A proper FE solution should converge (as the FE mesh is refined) to the exact solution [1]. Refinement means that the object is subdivided into a gradually increasing number of smaller elements. For the assessment of the

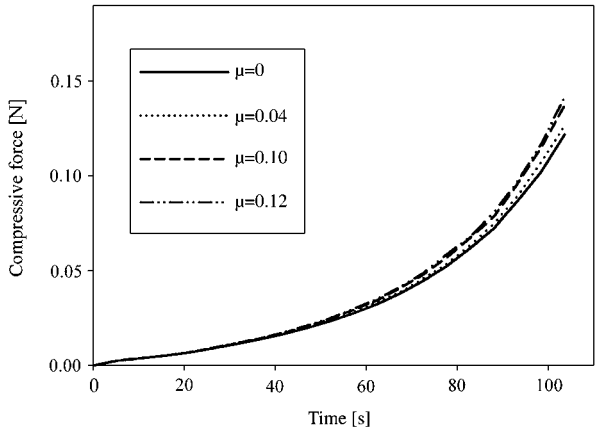

Figure 7 Influence of the friction parameter on the compressive force of the sample characterized by $\mathbf{p}_3$ (Table 2).

quality of our FE results, we started the refinement procedure from a cloud of points (Figure 1C) of a particular sample to create finer FE meshes. Upon mesh refinement, the maximal simulated force did not change by more than 2.3% force. Considering the high computational cost of the iterated FE calculations, the meshes of approximately 3000 elements were deemed to be sufficiently accurate.

In conclusion, the large range of mechanical parameters which were obtained from compression experiments on three uteri has been documented, and they characterize the mechanical behavior of uterine material under compression. Amended with corresponding values which are valid for extension (where anisotropy might have to be taken into account), our measurements and constitutive approach may contribute to a realistic simulation of the myometrium, which, for example, is useful for surgical training simulators.

Acknowledgements

This work was supported by the Swiss NSF Computer Aided and Image Guided Medical Interventions (NCCR CO-ME) project.

References

[1] Bathe K-J. Finite element procedures. London: Prentice-Hall International 1996.
[2] Chui C, Kobayashi E, Chen X, Hisada T, Sakuma I. Combined compression and elongation experiments and nonlinear modelling of liver tissue for surgical simulation. Med Biol Eng Comput 2004; 42: 787–798.
[3] Conrad JT, Johnson WL, Kuhn WK, Hunter CA. Passive stretch relationships in human uterine muscle. Am J Obstet Gynecol 1966; 96: 1055–1059.
[4] Conrad JT, Kuhn WK, Johnson WL. Stress relaxation in human uterine muscle. Am J Obstet Gynecol 1966; 95: 254–265.
[5] Conrad JT, Kuhn WK. Active length-tension relationship in human uterine muscle. Am J Obstet Gynecol 1967; 97: 154–160.
[6] Fung YC. Biomechanics: mechanical properties of living tissues. 2nd ed. New York: Springer 1993.
[7] Goerttler K. Der funktionelle Bau des menschlichen Uterus. Anat Anz 1929; 67: 122–130.
[8] Hartmann S, Neff P. Polyconvexity of generalized polynomial-type hyperelastic strain energy functions for near-incompressibility. Int J Solids Struct 2003; 40: 2767–2791.
[9] Holzapfel GA. Nonlinear solid mechanics: a continuum approach for engineering. 2nd ed. Chichester: Wiley 2000.
[10] Joelsson I. Mechanics of human myometrium studied with dynamic tests in vivo. Acta Obstet Gyn Scan 1972; 51: 127–135.
[11] Joelsson I, Gidlund L, Anzen B, Ingelmansundberg A. In vivo determination of stress-strain relation of human myometrium. Acta Obstet Gyn Scan 1976; 55: 325–331.
[12] Kauer M, Vuskovic V, Dual J, Szekely G, Bajka M. Inverse finite element characterization of soft tissues. Med Image Anal 2002; 6: 275–287.
[13] Mazza E, Nava A, Bauer M, Winter R, Bajka M, Holzapfel GA. Mechanical properties of the human uterine cervix: an in vivo study. Med Image Anal 2006; 10: 125–136.
[14] Miller K. Method of testing very soft biological tissues in compression. J Biomech 2005; 38: 153–158.
[15] Nava A, Mazza E, Kleinermann F, Avis NJ, McClure J, Bajka M. Evaluation of the mechanical properties of human liver and kidney through aspiration experiments. Technol Health Care 2004; 12: 269–280.
[16] Ogden RW. Non-linear elastic deformations (facsim. ed.). Mineola, NY: Dover Publications 1997.
[17] Pearsall GW, Roberts VL. Passive mechanical properties of uterine muscle (myometrium) tested in vitro. J Biomech 1978; 11: 167–176.
[18] Schofield BM, Wood C. Length-tension relation in rabbit and human myometrium. J Physiol Lond 1964; 175: 125–133.
[19] Spencer AJM. Continuum theory of the mechanics of fibre-reinforced composites. Wien: Springer 1984.
[20] Szekely G, Bajka M, Brechbuhler C, et al. Virtual reality based surgery simulation for endoscopic gynaecology. Stud Health Technol Inform 1999; 62: 351–357.
[21] Tschoegl NW. The phenomenological theory of linear viscoelastic behavior: an introduction. Berlin: Springer 1989.
[22] Van Loocke M, Lyons CG, Simms CK. A validated model of passive muscle in compression. J Biomech 2006; 39: 2999–3009.
[23] Weiss S, Jaermann T, Schmid P, et al. Three-dimensional fiber architecture of the nonpregnant human uterus determined ex vivo using magnetic resonance diffusion tensor imaging. Anat Rec A Discov Mol Cell Evol Biol 2006; 288: 84–90.
[24] Wetzstein R. Der Uterusmuskel: Morphologie. Arch Gynäkol 1965; 202: 1–13.
[25] Wood C. The expansile behaviour of the human uterus. J Obstet Gyn Br Comm 1964; 71: 615–620.
[26] Wu JZ, Dong RG, Schopper AW. Analysis of effects of friction on the deformation behavior of soft tissues in unconfined compression tests. J Biomech 2004; 37: 147–155.
[27] Wu JZ, Dong RG, Smutz WP. Elimination of the friction effects in unconfined compression tests of biomaterials and soft tissues. P I Mech Eng H 2004; 218: 35–40.

Received December 13, 2006; accepted December 14, 2007